

## A SPECTRAL-LINE SURVEY OF W51 FROM 17.6 TO 22.0 GHz

M. B. BELL, L. W. AVERY, AND J. K. G. WATSON

Herzberg Institute of Astrophysics, National Research Council of Canada, 100 Sussex Drive, Ottawa, Canada, K1A 0R6

*Received 1992 July 30; accepted 1992 September 30*

## ABSTRACT

The complete centimeter-wave spectrum between 17.57 and 22.04 GHz of the W51Main/South complex has been surveyed with the NRAO 140 foot (43 m) telescope with channel spacings of 0.3125 MHz and down to a  $1\sigma$  level between  $T_A = 1\text{--}5$  mK. Approximately 224 lines were detected, of which 94 are hydrogen or helium recombination lines, 11 are ammonia lines, 19 are coincident with known molecular transitions, and 100 are unidentified. Observations obtained with longer integration times, but over very limited frequency ranges, indicate that many of the known molecules might be detectable in this source with only a few hours of integration time. The carbon chain molecules more common in other sources ( $C_nH$ ,  $C_nN$ ,  $HC_nN$ , etc.) are not strong, although  $HC_3N$ ,  $HC_5N$  and several nonlinear molecules containing  $C_3$  appear to have been detected.

Based on the high signal-to-noise ratio obtained for  $C_3H_2$  lines, and the fact that the off-axis  $^{13}C$  isotopomer was also detected, we have concluded that W51 is probably an excellent source in which to search for propargylene, the nearly linear version of this molecule.

Eleven transitions of ammonia from (4,2) to (14,11) were also detected in the survey and appear to show an increase in excitation temperature with both  $J$  and  $(J - K)$  for this molecule.

*Subject headings:* ISM: individual (W51) — line: identification — radio lines: atomic — radio lines: ISM

## 1. INTRODUCTION

W51 is a complex in the Sagittarius spiral arm made up of several H II regions and molecular clouds. It is one of the most luminous star-forming regions in the Galaxy, containing clusters of  $H_2O$  masers, molecular hydrogen emission, and knots of hot  $NH_3$  gas (Martin 1972; Genzel et al. 1982; Beckwith & Zuckerman 1982; Ho, Genzel, & Das 1983).

Although spectral surveys of several different sources have been carried out at millimeter wavelengths (Turner 1989 and references therein; Avery et al. 1992) no extensive, sensitive, centimeter-wave surveys have so far been published. Since many new, unidentified lines have been detected in our survey of W51, we present these data in the hope that the carriers of these lines, which may include new interstellar molecules, might be identified.

## 2. OBSERVATIONS

The observations were made with the 43 m telescope of the National Radio Astronomy Observatory<sup>1</sup> and were mainly carried out during 1990 February, with the remaining 10% completed in 1991 January. For all observations the telescope was centered on the position  $\alpha = 19^h21^m26^s$ ,  $\delta = 14^\circ24'35''$  (1950.0). The beamwidth at these frequencies is  $\sim 1.4$ . At all frequencies it was sufficiently large to cover the entire W51Main/South complex which includes both W51 IRS 1 and the W51-e1 and W51-e2 regions (see, e.g., Ho et al. 1983). Since the beam could not cover both W51 IRS 1 and W51 IRS 2 simultaneously, the former was chosen because the results of Fomalont & Weliachew (1973) suggest that the density of the

molecular cloud increases eastward from IRS 2 to IRS 1. The telescope meridian aperture efficiency also varied slightly across the survey frequency range, but was  $\sim \eta_A = 0.30 \pm 0.03$ . The beam efficiency,  $\eta_B = 0.4 \pm 0.04$ . An LSR velocity of  $60 \text{ km s}^{-1}$  was assumed throughout. However, it is apparent from the data that the velocity obtained from the recombination lines and the stronger molecular lines is closer to  $58 \text{ km s}^{-1}$ . The velocity obtained from the ammonia transitions detected, on the other hand, was closer to  $63 \pm 3 \text{ km s}^{-1}$ .

Observations were made only under good or excellent observing conditions. The data have not been corrected for antenna gain variations as a function of hour angle, telescope efficiency, or atmospheric attenuation, except as indicated in the ammonia analysis. Pointing checks were made every 2 hr using standard pointing sources, and calibration was accomplished by means of a noise tube.

The observing technique used was a combination of both frequency switching and position switching. Initially, a series of 4 minute on-source integrations, interwoven with a series of 4 minute off-source integrations was carried out for 2 hr at each frequency. An additional 1–2 hours of integration was obtained as necessary, depending on system temperature and observing conditions. During each “on” and “off” integration the frequency was switched each second using offsets of  $\pm 3$  channels (one channel = 0.3125 MHz). These offsets can thus accommodate line widths of  $\sim 25\text{--}32 \text{ km s}^{-1}$  over the survey range. The off-source subtraction was found to be necessary to avoid spectral contamination by atmospheric lines (see Bell & Feldman 1991) and the off-source position was chosen to allow the “off” integration to start at the same hour angle as the “on.” Focus modulation was used to cancel the fundamental ripple produced by the telescope surface-to-subdish reflection. Additional integration (up to 8 hr on source) was obtained over several limited frequency ranges where the line density

<sup>1</sup> The National Radio Astronomy Observatory (NRAO) is operated by Associated Universities, Inc., under cooperative agreement with the National Science Foundation.

appeared to be particularly high (e.g., 18265–18545 MHz, 20785–20955 MHz, 21555–21695 MHz). Before overlapping, the main and reference lines appear side-by-side, one upright, the other inverted. The offset was kept as small as possible in order to achieve flat baselines after overlapping, which is not a trivial problem when the source has a strong continuum flux.

Spectra were obtained with the NRAO autocorrelation spectrometer split into two 80 MHz banks, each containing 256 channels. With frequency overlaps of 10 MHz, each window was thus 140 MHz wide.

Data reduction was carried out using PCPOPS and DRAW-SPEC running on a 386AT PC where, after averaging, it was a simple matter to clean the resulting overlapped line signature of its reference components before fitting Gaussians (see Bell & Feldman 1991 for a more detailed description of this technique). Since the full width of the hydrogen recombination lines was slightly greater than allowed for by the offsets of  $\pm 3$  channels, and because the frequency-switching offset was fixed while the frequency width of the lines varied across the survey range, a decrease of a few percent in the amplitudes of the broad recombination lines with increasing frequency was anticipated. It should be noted, however, that the error introduced by this effect was still much smaller than the sum of the uncertainties introduced by the calibration, the reduction of telescope efficiency with increasing frequency, and atmospheric absorption near the water line.

The sensitivity also varied by at least a factor of 2 across the survey because of variations in the receiver performance with frequency. Only in the narrow frequency range between 18050 and 18100 MHz, near the SiS ( $J = 1-0$ ) line, was the receiver passband severely degraded. Because of the special observing and data reduction techniques used, no baseline ripples with periods longer than six channels (twice the frequency-switched offset) will remain in the data. We have also found that for long integration periods ( $\sim 30$  hr) no ripples of any period with amplitudes in excess of  $3\sigma$  are present in the averaged data (Bell et al. 1993). However, for 2 hr integrations, the possibility still exists that some of the low-level features in the spectra might be ripple related, especially if several occur side-by-side. We feel, on the other hand, that isolated weak features are less likely to be spurious. Local or satellite interference, unless it varies rapidly, is expected to disappear with off-source subtraction. In W51 the recombination lines have halfwidths (FWHM) slightly larger than the normal thermal width of  $25 \text{ km s}^{-1}$ , while the molecular lines are narrower and seldom exceed  $\sim 12 \text{ km s}^{-1}$ .

### 3. RESULTS

In Figure 1 we present the entire frequency survey plotted so that weak lines ( $T_A \sim 10 \text{ mK}$ ) are visible. The wide lines in the spectrum are due to recombination lines of atomic hydrogen and it is apparent that lines with  $\Delta n$  in excess of 8 can be seen in the more sensitive regions of the band after integrations of a few hours. Unidentified lines thought to be real and molecular in origin are labeled *U*-frequency. Those that are tentative detections needing confirmation are labeled *T*-frequency. It should be noted, however, that for the weakest lines it is very difficult to determine which category is more appropriate, and

some of those labeled *U*-frequency will undoubtedly turn out to be spurious. A complete listing of the frequencies of all lines is presented in Table 1. In Figure 2 we present those molecular lines that extend off-scale in Figure 1 plotted so the full extent of each line can be seen.

Using the H ( $\Delta n = 1$ ) lines between 18 and 25 GHz it is possible to obtain a snapshot of the reduction in antenna temperature due to the combined effect of telescope efficiency and atmospheric absorption near the water line. Orion A data obtained in this way over a 30 minute interval were used in the ammonia reduction process to correct for these effects, but no correction was applied to the data in Figure 1 or in Table 1, and the reader should therefore keep in mind that the lines above  $\sim 20$  GHz will be increasingly reduced by the combined effects of the decrease in telescope efficiency and the increasing atmospheric absorption. A comparison of the relative strengths of the H ( $\Delta n = 1$ ) lines detected in the W51 survey and from Orion A revealed that there was an error in the noise tube calibration of  $\sim 30\%$  near 18.0 GHz where the receiver response is poor. For the most part, however, calibration errors were less than 10%. However, for frequencies above 20 GHz it is apparent that changes in atmospheric absorption can introduce significant uncertainties even in relatively good weather conditions. Since accurate calibration of each 80 MHz window was beyond the scope of this survey we have undertaken a separate set of accurately calibrated observations of W51 for the purpose of examining the recombination lines in this source (Bell et al. 1993), and no further discussion of recombination lines will be carried out here.

The data have not been smoothed, but since the full velocity width of the H recombination lines is slightly greater than that allowed for by the frequency-switching offset, the resulting line shapes may have been affected by the frequency-switching technique used (see Bell & Feldman 1991). For most lines the peak values are not expected to be affected. It is important to note, however, that this technique can introduce some uncertainty in the line strengths due to the CLEAN process when lines are so closely spaced that one line falls in the CLEAN area of another. In this case the relative strengths of the lines depends on the sequence in which they are cleaned. No error in the position of the lines is introduced. Throughout the reduction process, when closely spaced lines were cleaned, the sequence followed was from strong to weak lines. Accurate line strengths for closely spaced lines will therefore require further observations using a different technique. Lines that fit into this category have been included with those lines labeled *T*-frequency in Table 1. It should be noted that the CLEAN program does not use a conventional “clean” algorithm but relies simply on the assumption that the location and amplitude of the “ghost” images are known and can be removed using a scaled version of the line being cleaned. Thus the CLEAN process cannot create false lines except inside the overlap region which is always quite close to the line being cleaned.

When the lines detected in the spectrum of W51 are classified broadly according to strength there are some noticeable differences between the line content of this source and that of Orion (our unpublished data). Aside from the fact that ammonia is excited to much higher levels in Orion, the most striking feature is that in W51 the carbon ring molecule  $\text{C}_3\text{H}_2$  is very strong, and because of its line width, which is narrow enough

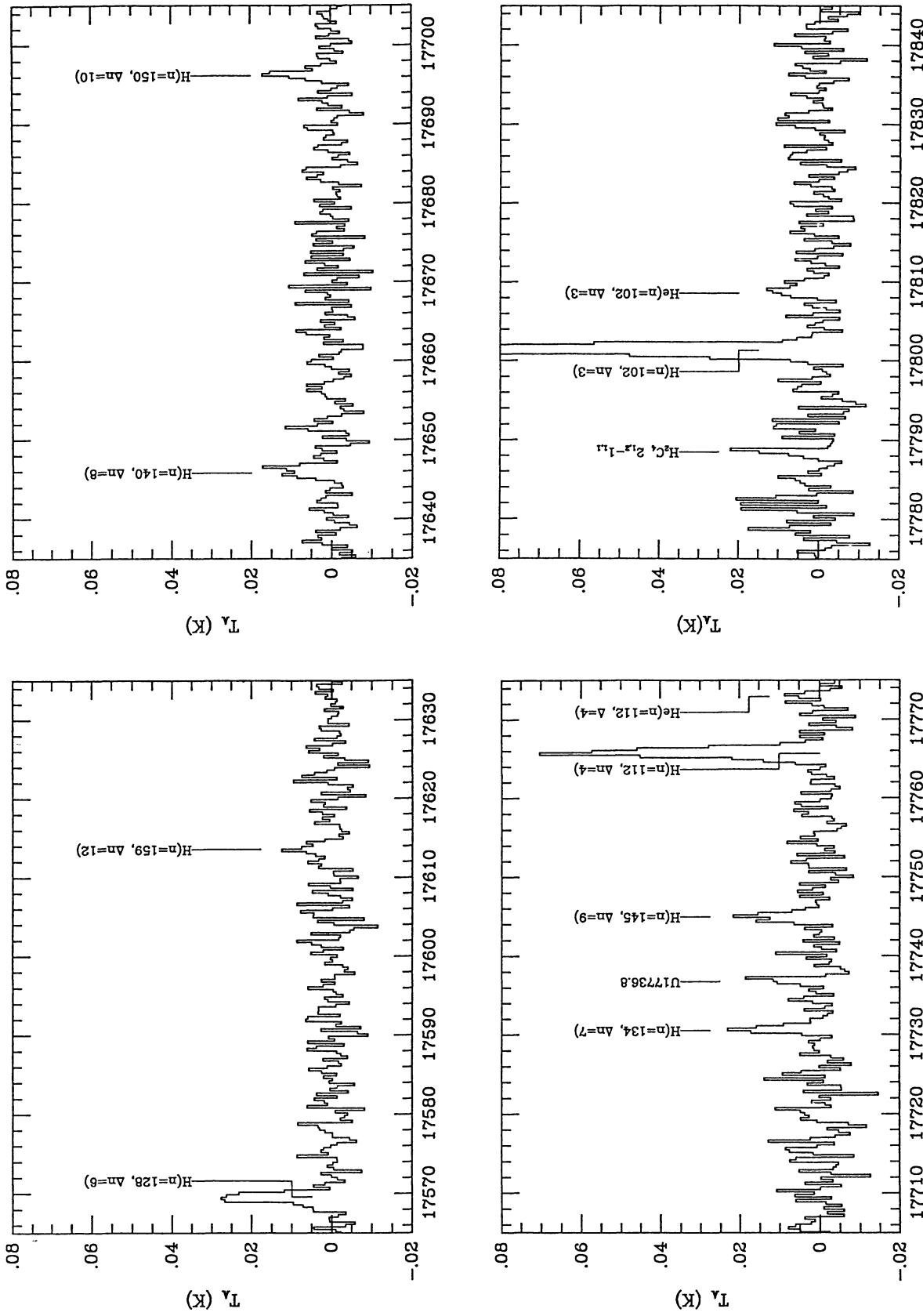


FIG. 1.—Complete spectral scan of W51 between 17.57 and 22.04 GHz presented so that weak lines ( $T_A \approx 10 \text{ mK}$ ) are visible. Unidentified lines thought to be real and molecular in origin are labeled  $U$ -frequency. Those labeled  $T$ -frequency are tentative detections needing confirmation. For lines whose rest frequencies are known the vertical bar indicates the expected position of the line assuming an LSR velocity of  $60 \text{ km s}^{-1}$ . For unidentified lines the vertical bar represents the line center for this LSR velocity. The temperature scale is uncorrected. The horizontal scale gives the frequency in MHz.

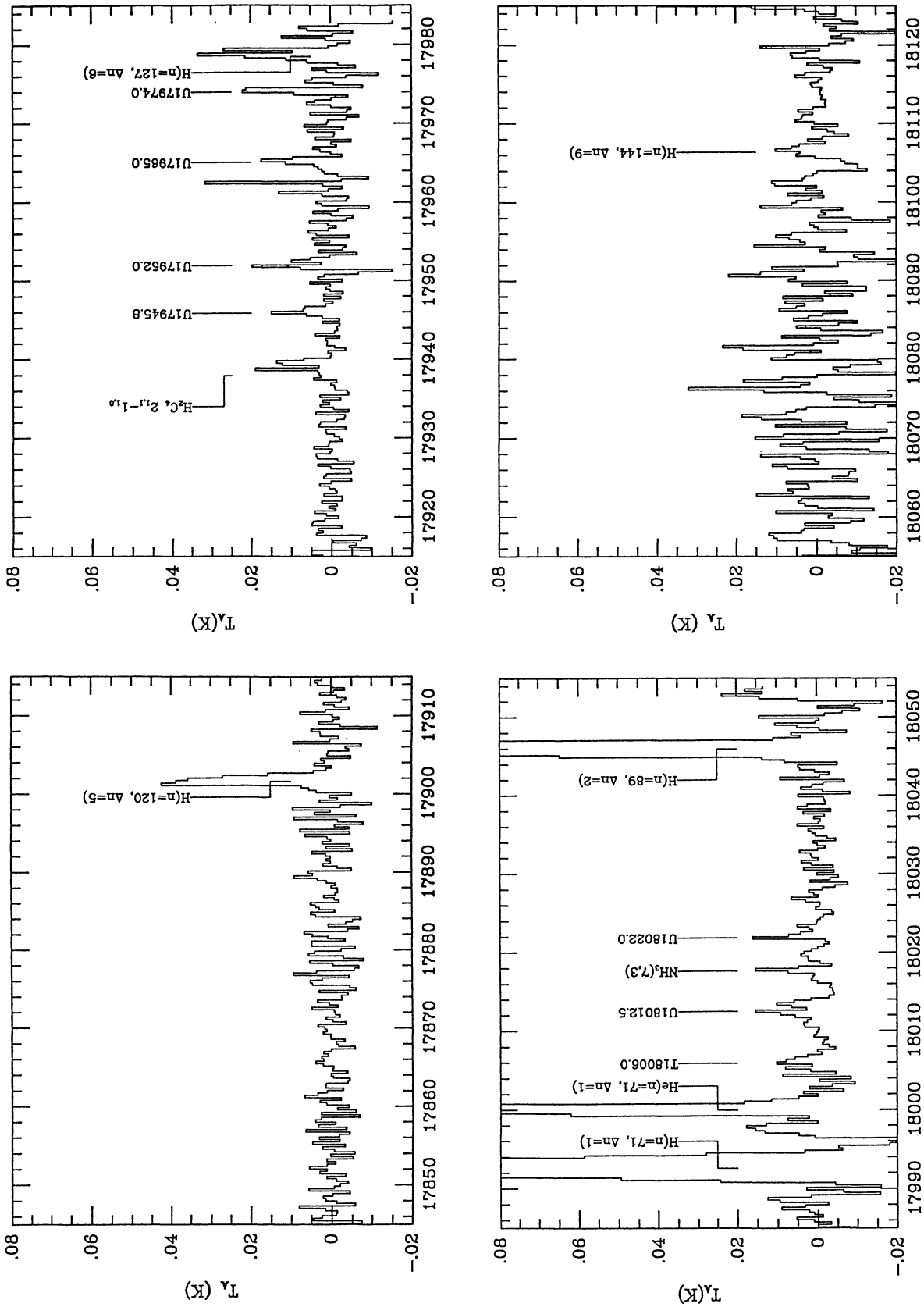


FIG. 1—Continued

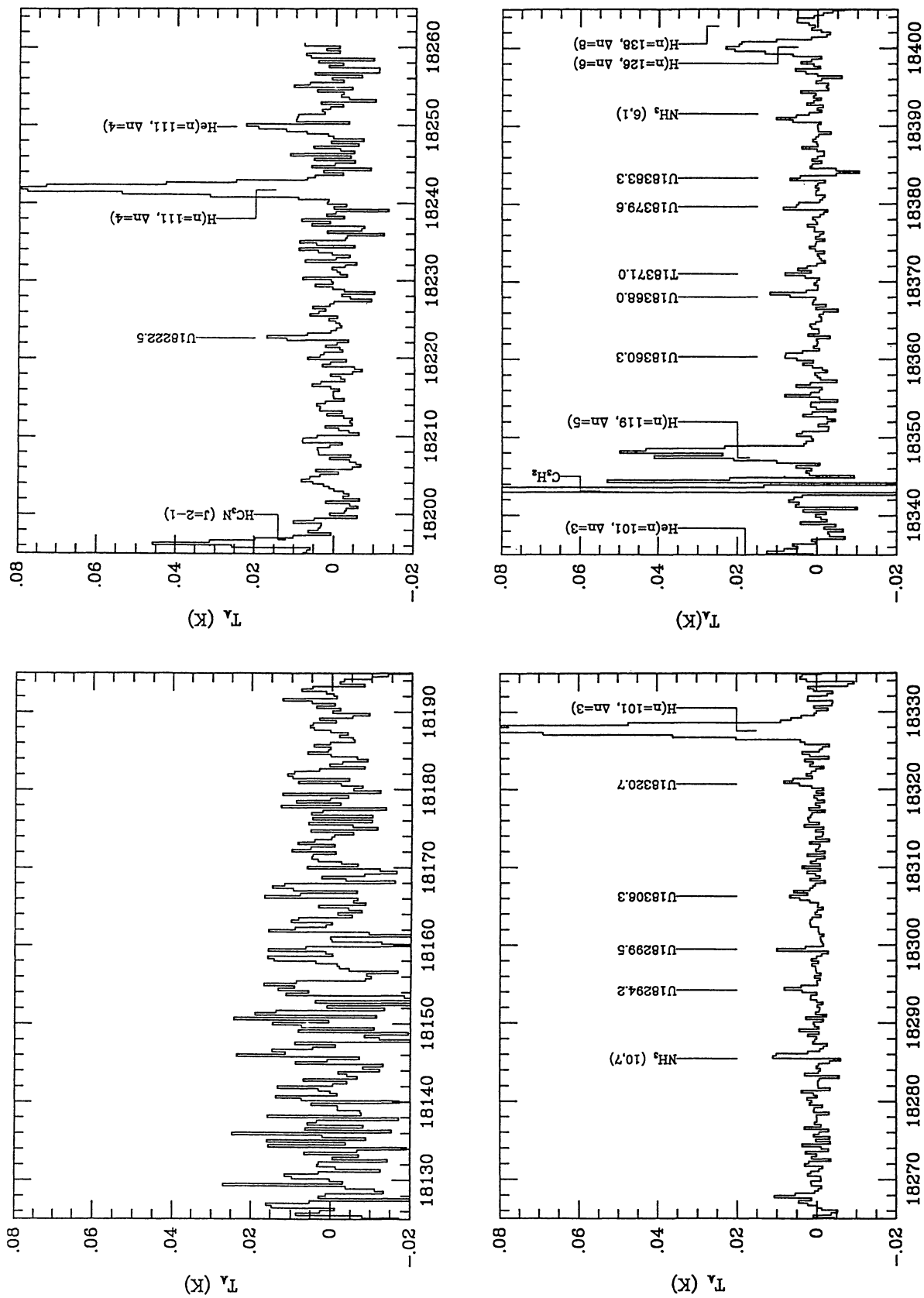


FIG. 1—Continued

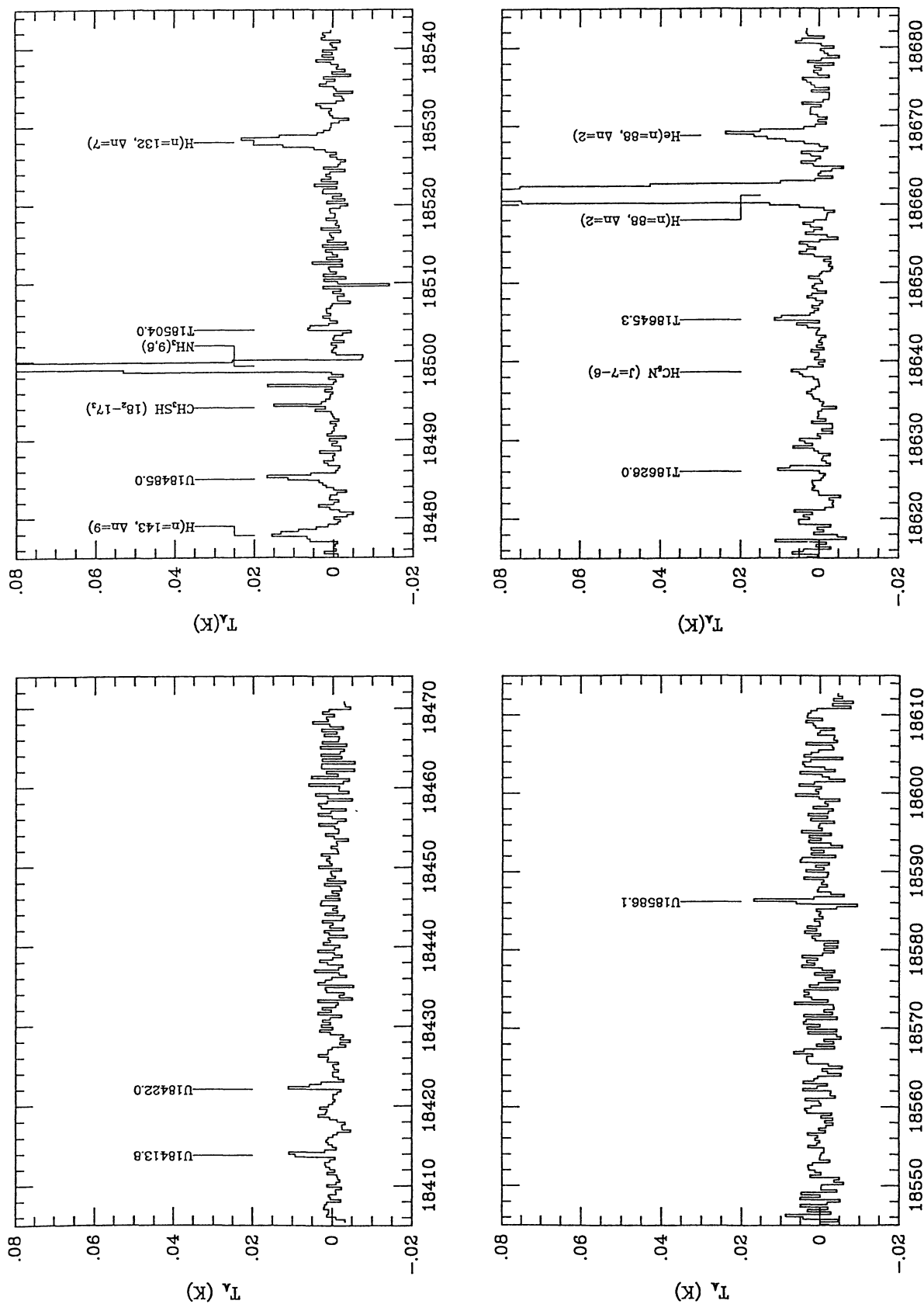


FIG. 1—Continued

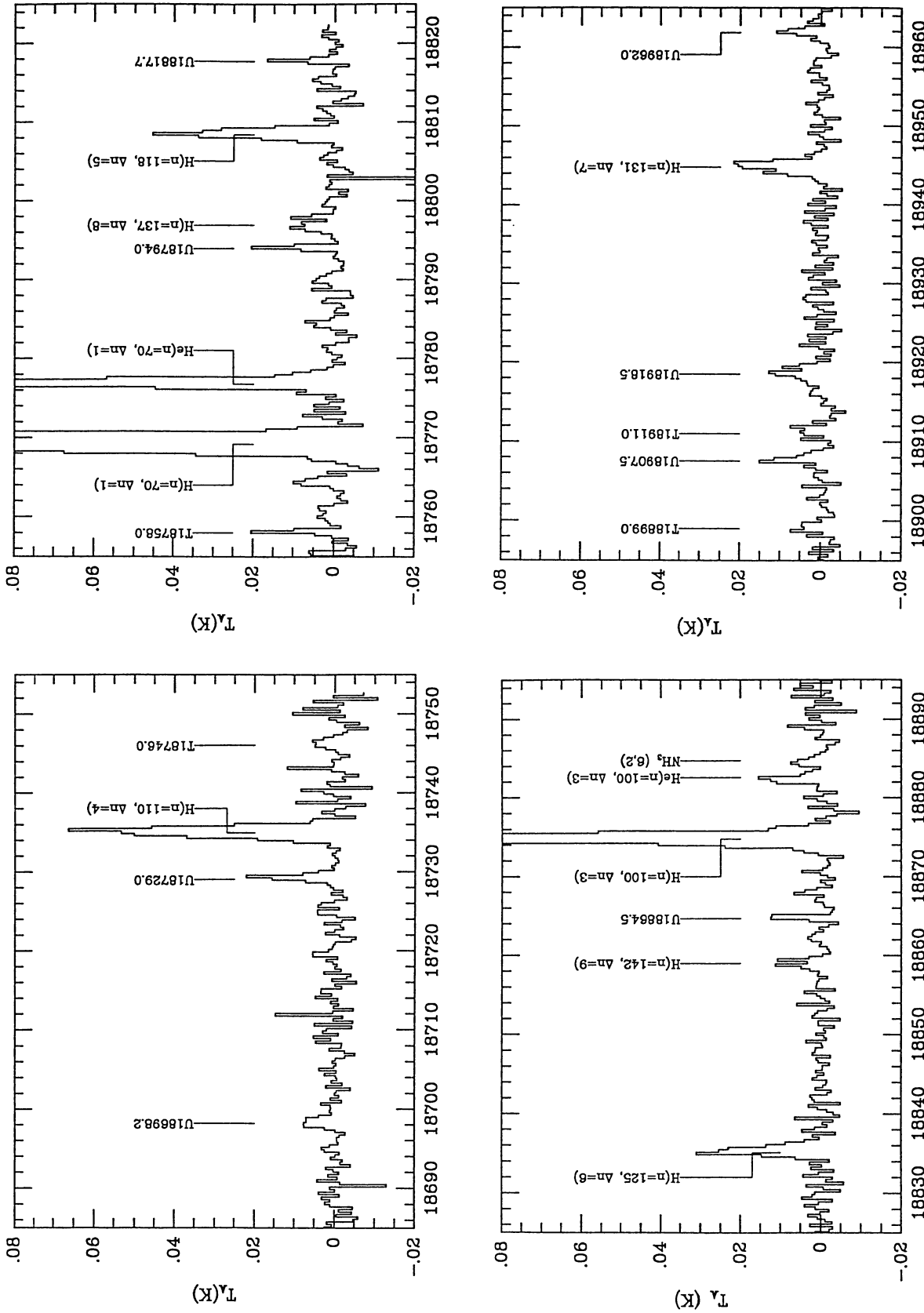


FIG. 1—Continued

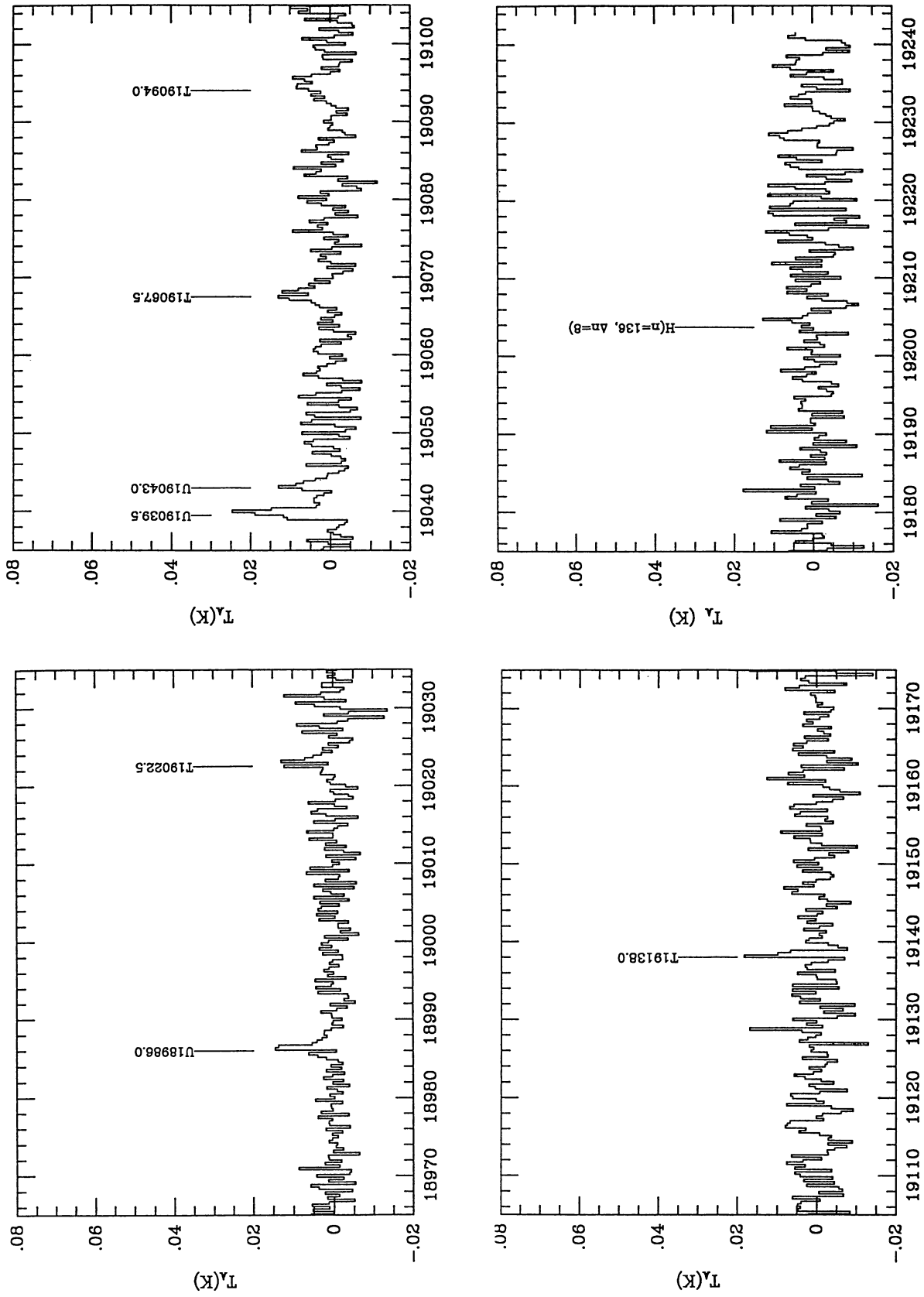


FIG. 1—Continued

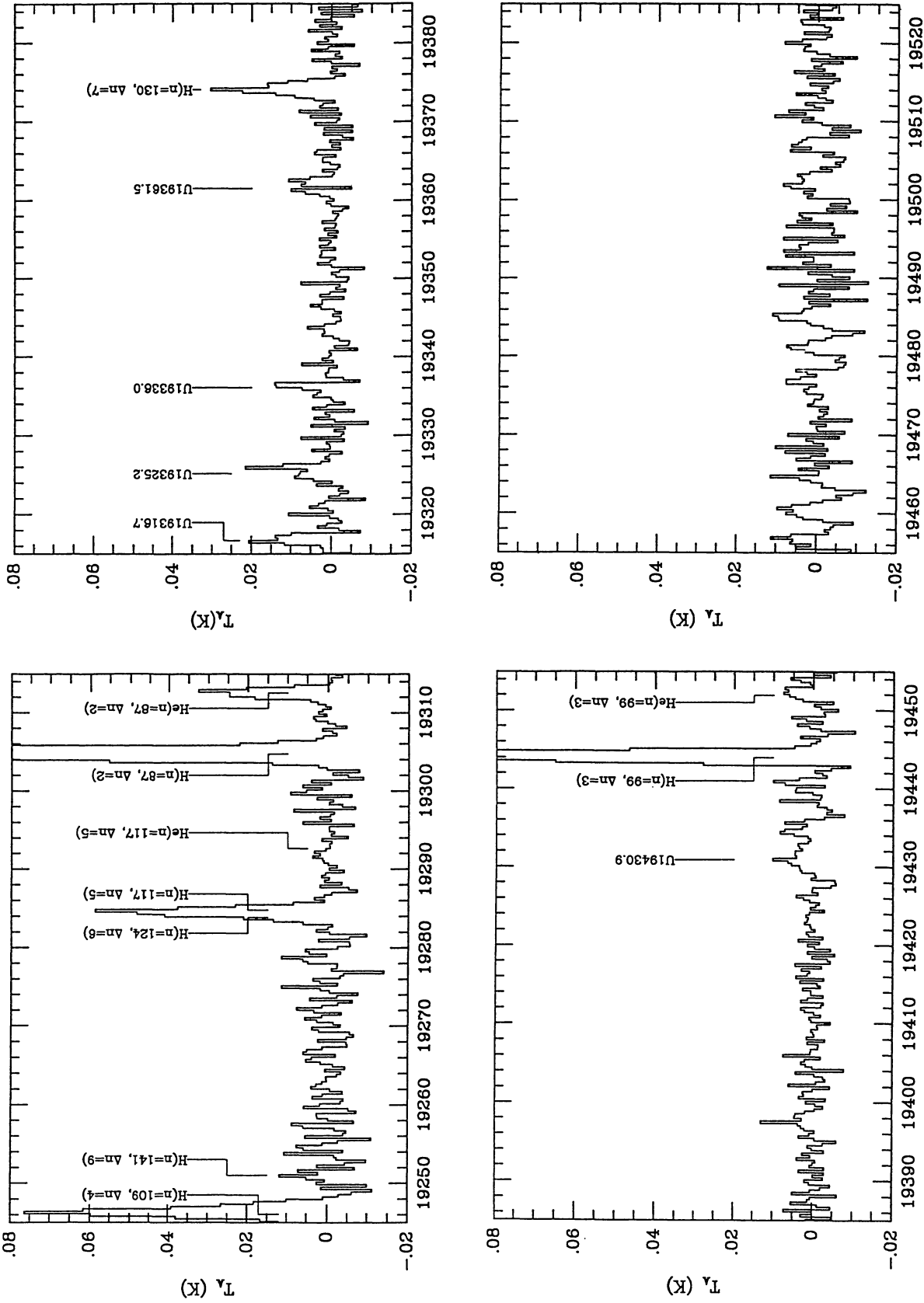


FIG. 1—Continued

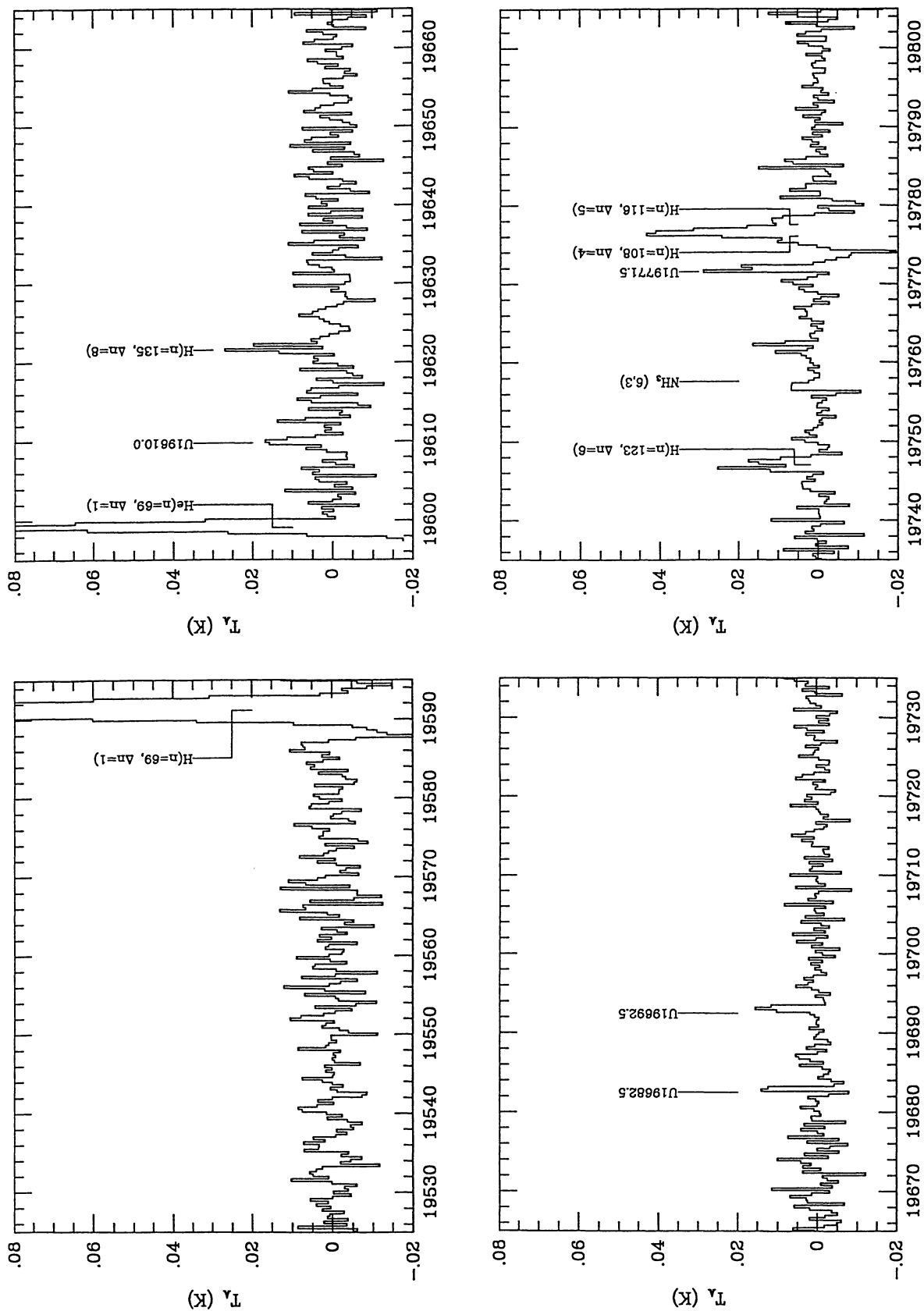


FIG. 1—Continued

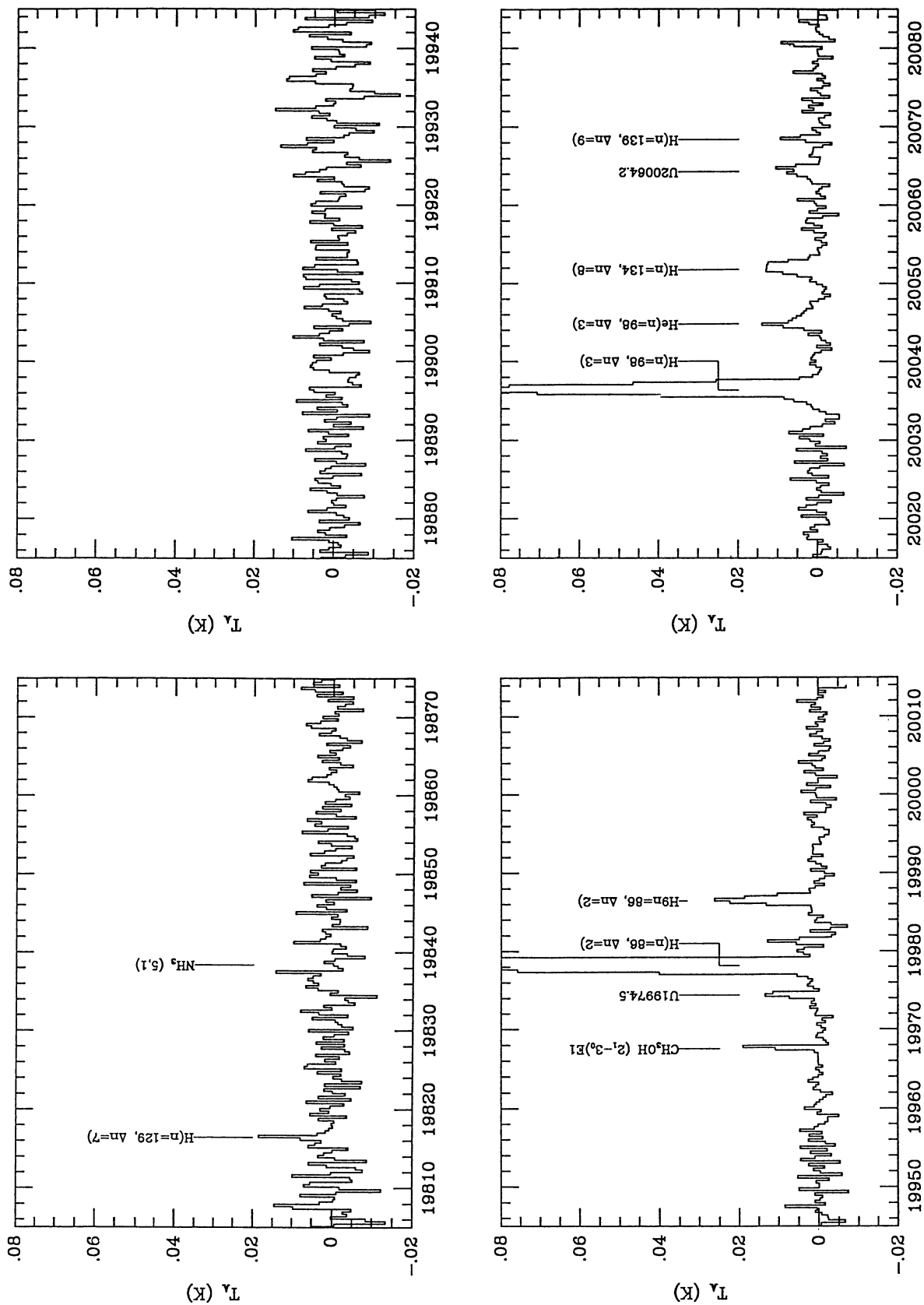


FIG. 1—Continued

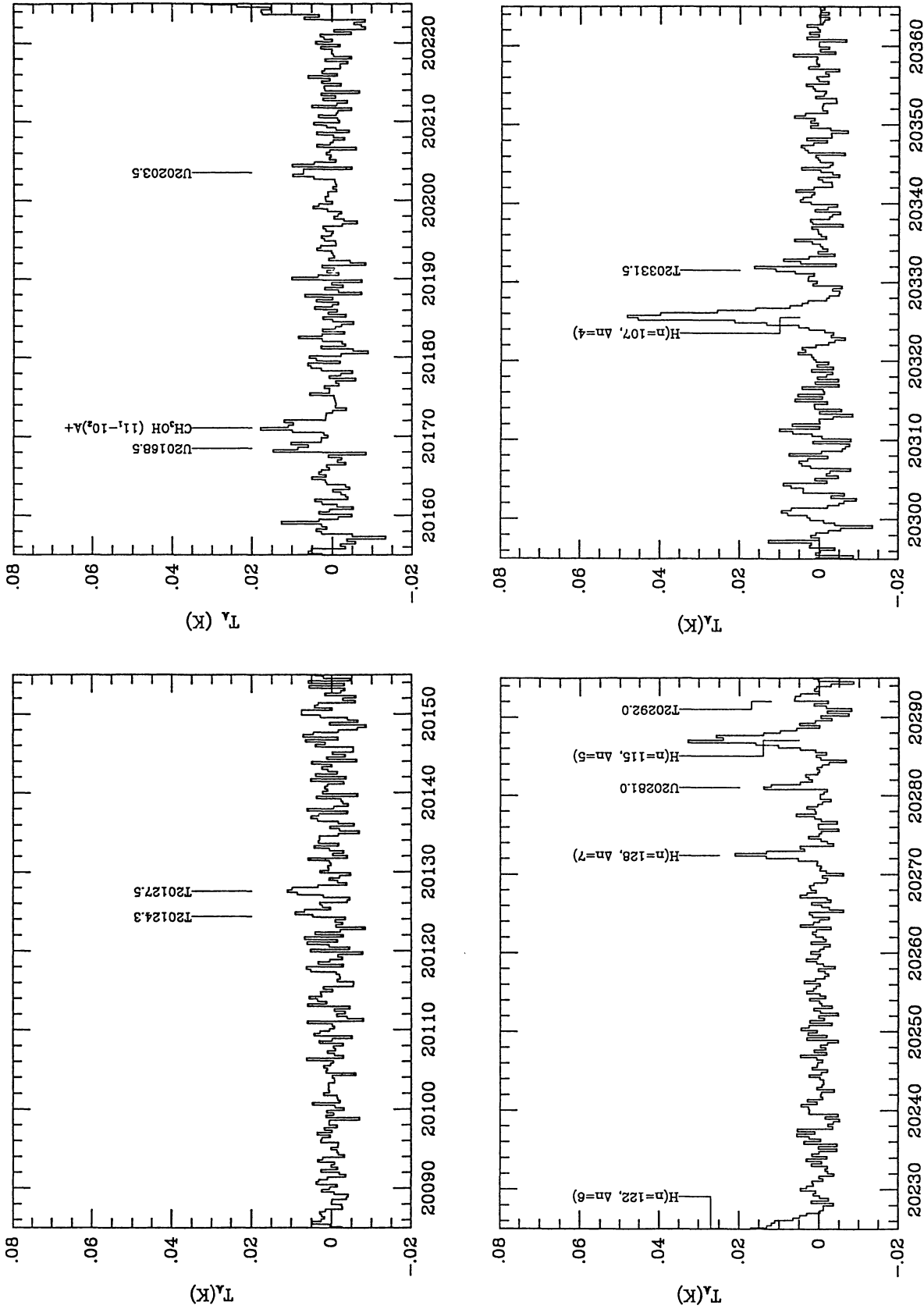


FIG. 1—Continued

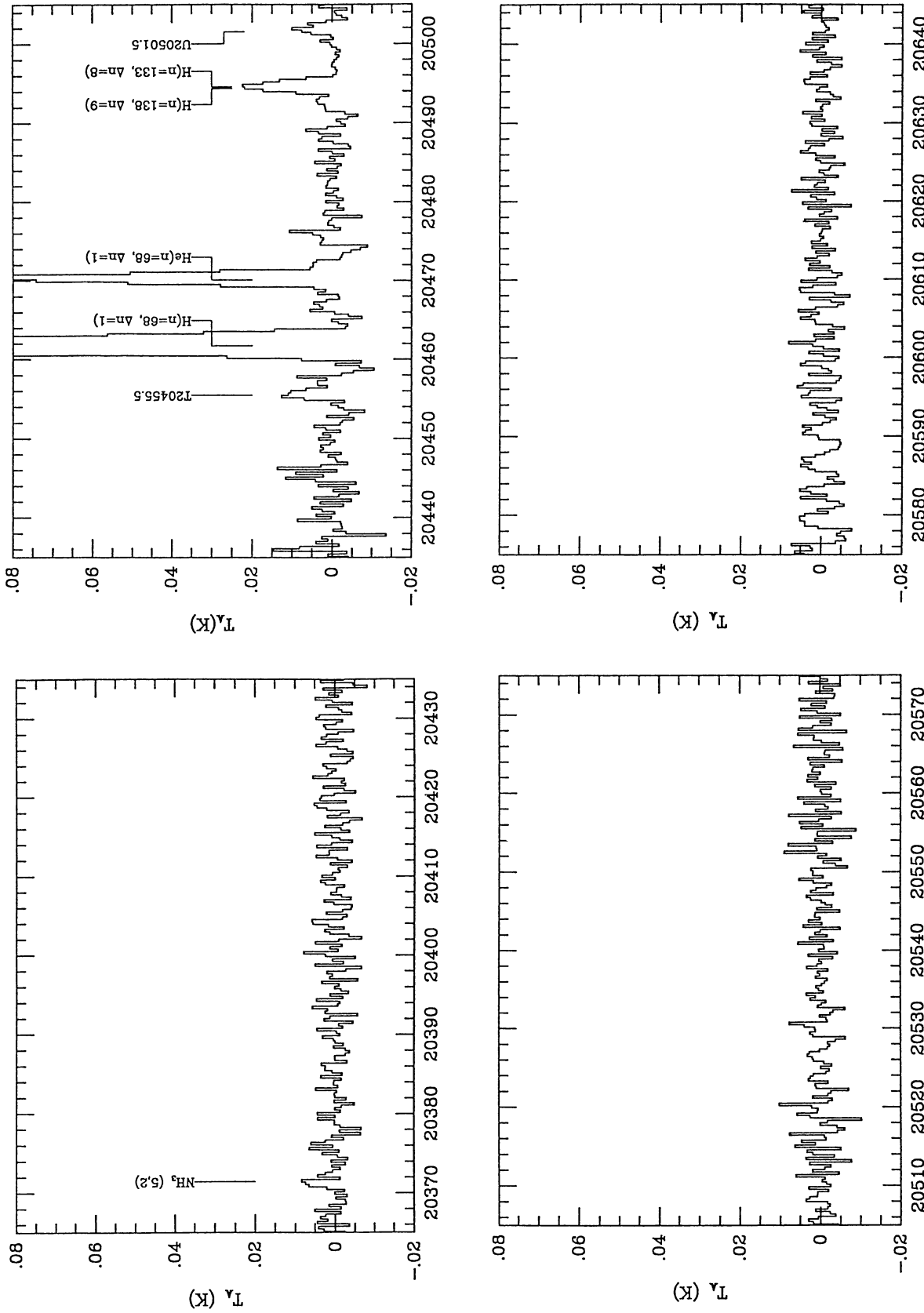


FIG. 1—Continued

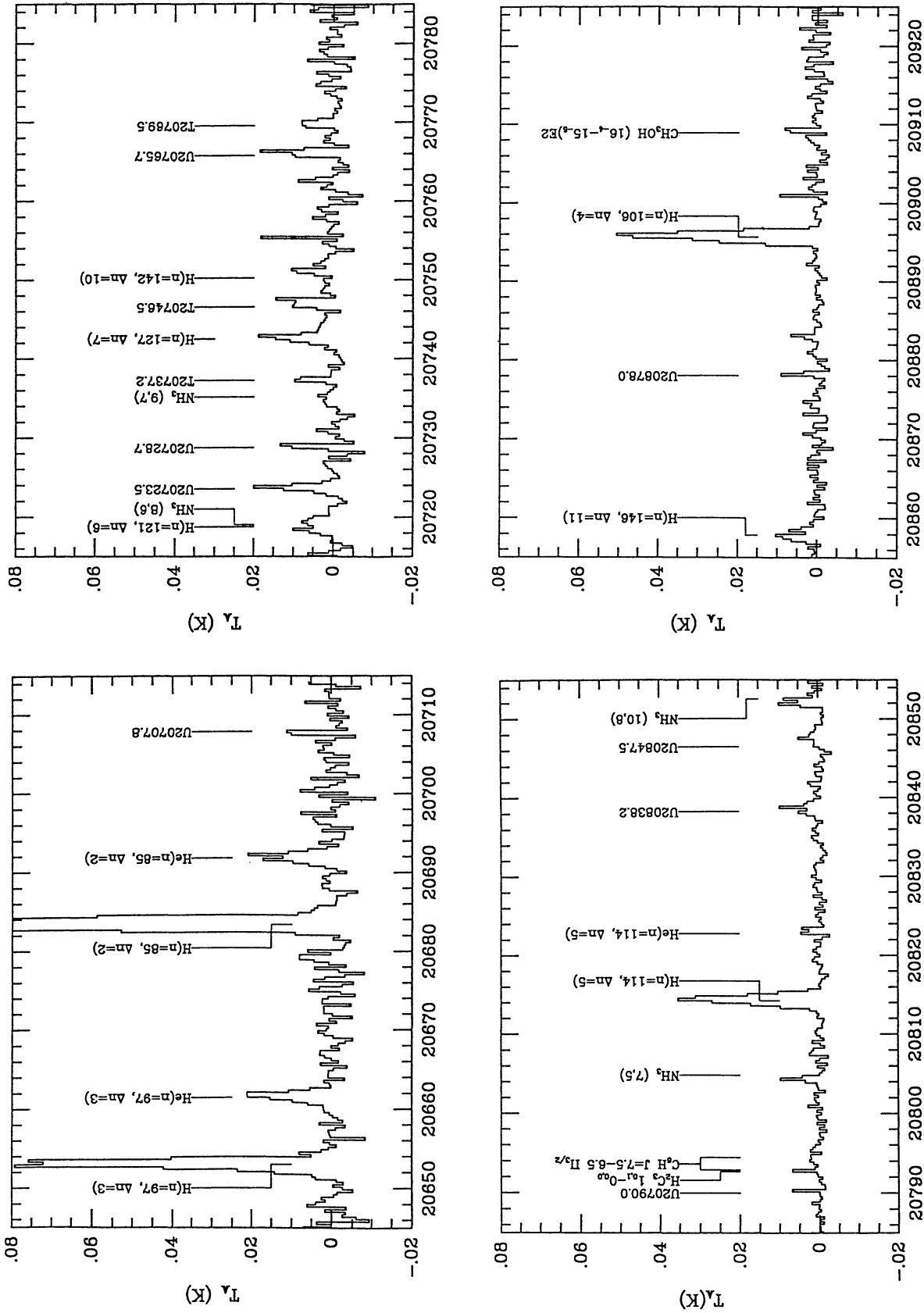


FIG. 1—Continued

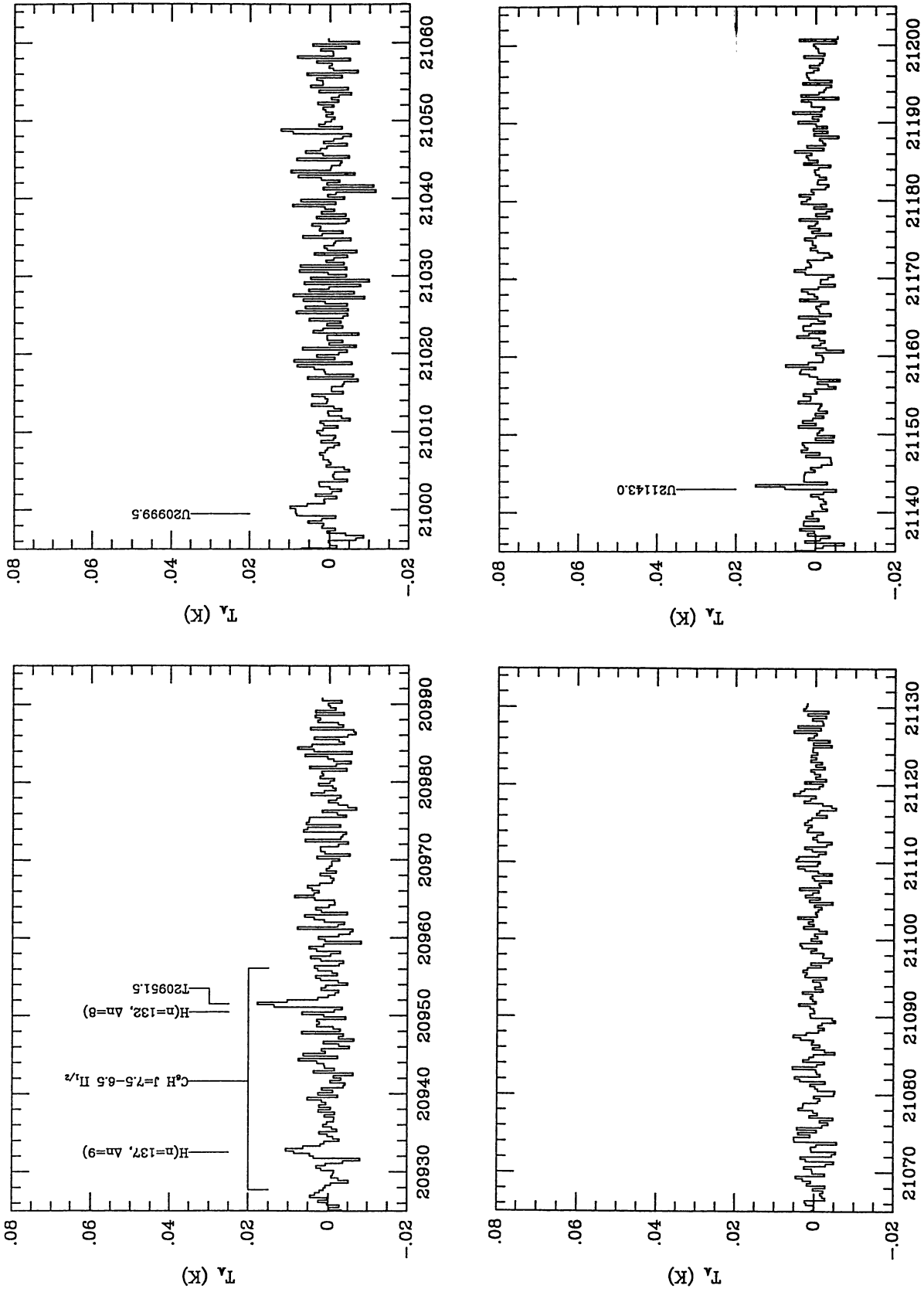


FIG. 1—Continued

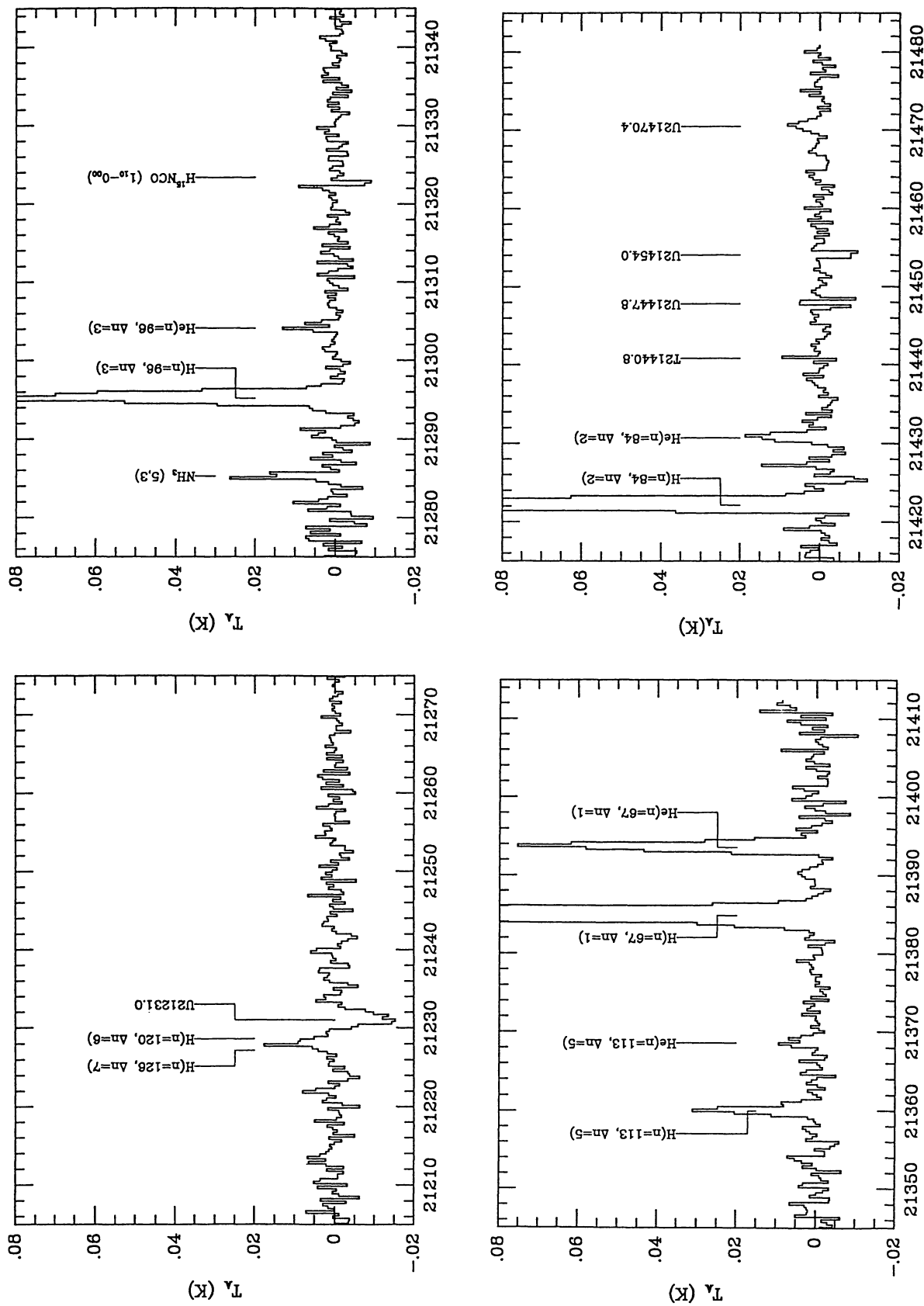


FIG. 1—Continued

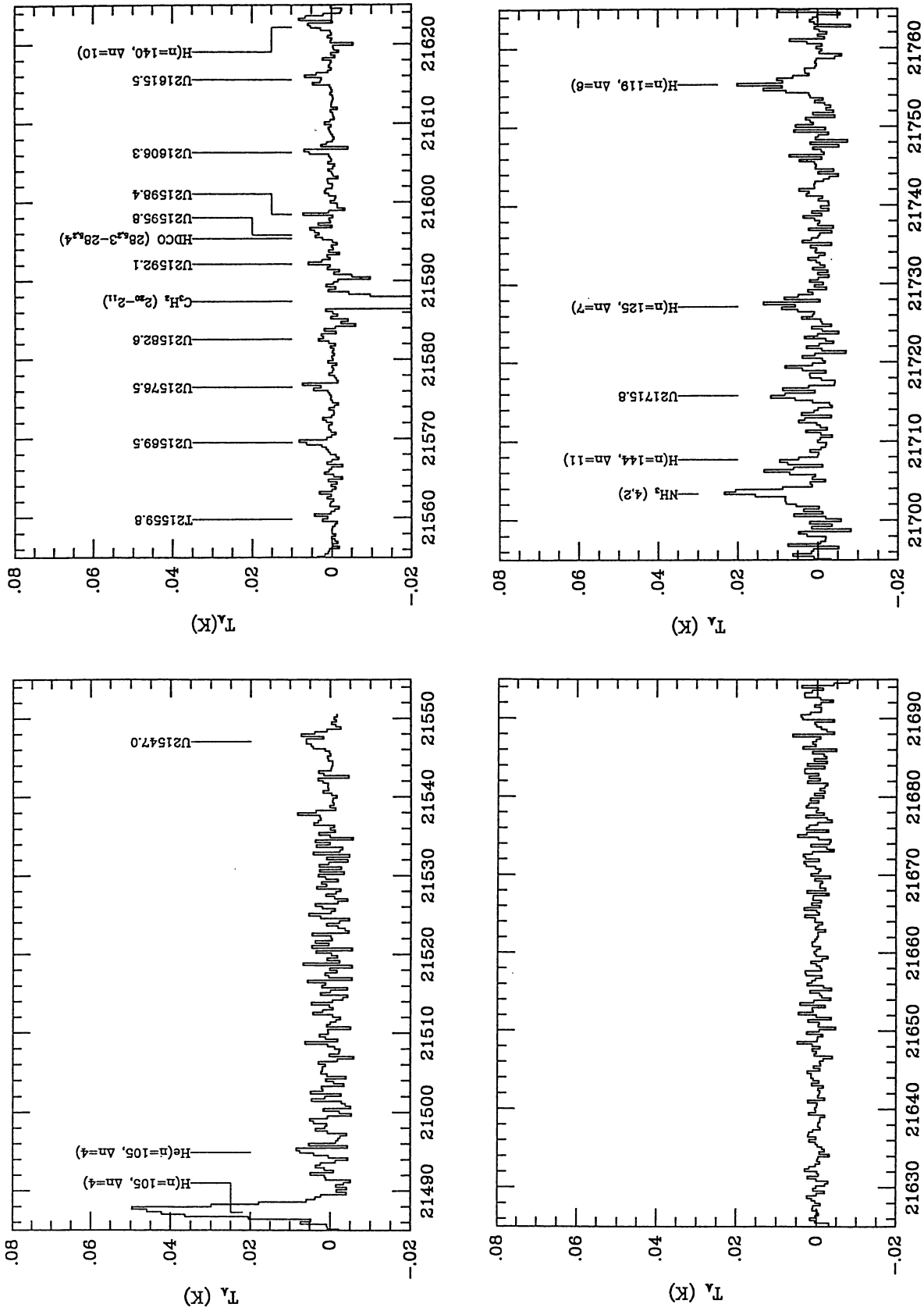


FIG. 1—Continued

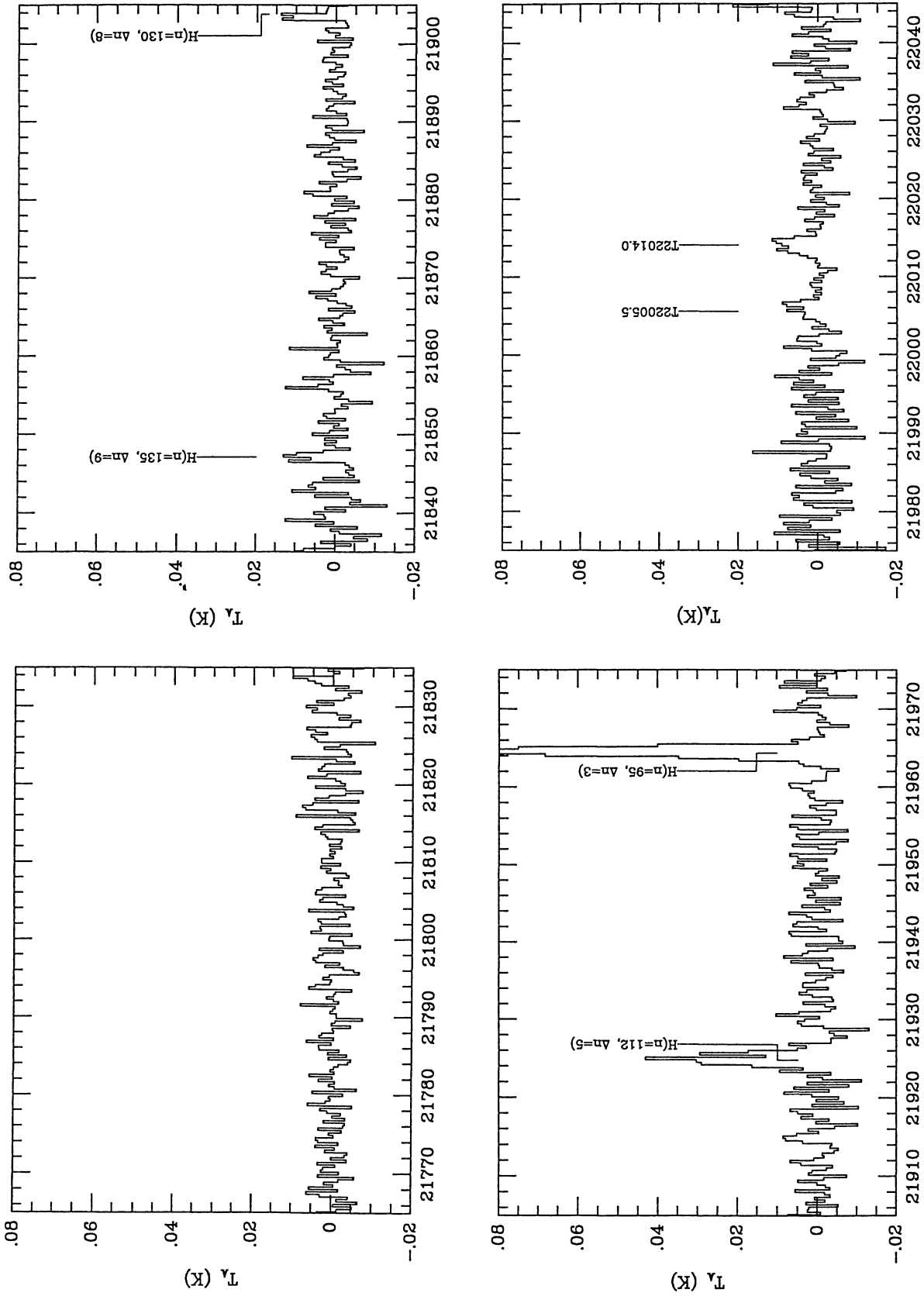


FIG. 1—Continued

TABLE 1  
LINES DETECTED IN W51 SPECTRAL SURVEY

Frequency (MHz)	$T_A$ (K)	Identification	Comments	Frequency (MHz)	$T_A$ (K)	Identification	Comments
17569.33	0.029	H(n=128, $\Delta n=6$ )		18874.72	0.1339	H(n=100, $\Delta n=3$ )	
17613.38	0.0099	H(n=159, $\Delta n=12$ )?		18882.54	0.0103	He(n=100, $\Delta n=3$ )	
17645.98	0.0138	H(n=140, $\Delta n=8$ )		18884.50	0.006	NH <sub>3</sub> (6,2)	
17696.17	0.0164	H(n=150, $\Delta n=10$ )		18899.0	0.005	T18899.0	
17730.5	0.023	H(n=134, $\Delta n=7$ )		18907.54	0.0134	U18907.5	
17736.75	0.017	U17736.8		18911.0	0.005	T18911.0	
17744.76	0.019	H(n=145, $\Delta n=9$ )		18918.50	0.0105	U18918.5	
17765.62	0.065	H(n=112, $\Delta n=4$ )		18944.72	0.0208	H(n=131, $\Delta n=7$ )	
17788.43	0.0209	H <sub>2</sub> C <sub>4</sub> 2 <sub>1,2</sub> -1 <sub>1,1</sub>	Ortho	18961.79	0.0108	U18962.0	
17801.26	0.1258	H(n=102, $\Delta n=3$ )		18986.20	0.0130	U18986.2	
17808.85	0.0117	He(n=102, $\Delta n=3$ )		19022.5	0.007	T19022.5	
17901.51	0.0422	H(n=120, $\Delta n=5$ )		19039.50	0.020	U19039.5	
17939.01	0.0121	C <sub>2</sub> H <sub>4</sub> 2 <sub>1,1</sub> -1 <sub>1,0</sub>	Ortho; H(n=158, $\Delta n=12$ ) at 17938.3 also	19043.0	0.010	U19043.0	
17945.85	0.0128	U17945.8		19067.5	0.010	T19067.5	
17951.95	0.0116	U17952.0		19094.0	0.007	T19094.0	
17965.09	0.017	U17965.0		19138.0	0.015	T19138.0	
17974.01	0.0267	U17974.0		19245.91	0.0638	H(n=109, $\Delta n=4$ )	
17978.61	0.0269	H(n=127, $\Delta n=6$ )		19284.12	0.0353	H(n=117, $\Delta n=5$ )	blended with H(n=124, $\Delta n=6$ ) at 19283.84
17992.58	1.3841	H(n=71, $\Delta n=1$ )		19304.67	0.2553	H(n=87, $\Delta n=2$ )	
17999.94	0.1663	He(n=71, $\Delta n=1$ )		19312.39	0.0649	He(n=87, $\Delta n=2$ )	
18005.89	0.0085	T18006.0		19316.70	0.013	U19316.7	
18012.46	0.0094	U18012.5		19325.20	0.007	U19325.2	
18017.62	0.0153	NH <sub>3</sub> (7,3)		19336.10	0.014	U19336.0	
18021.86	0.0691	U18022.0		19361.50	0.008	U19361.5	
18045.89	0.2759	H(n=89, $\Delta n=2$ )		19374.03	0.023	H(n=130, $\Delta n=7$ )	
18106.52	0.009	H(n=144, $\Delta n=9$ )	data questionable	19430.85	0.005	U19430.9	
18196.20	0.0398	HC <sub>3</sub> N (J=2-1)		19443.98	0.1429	H(n=99, $\Delta n=3$ )	
18222.65	0.0167	U18222.5		19452.12	0.0078	He(n=99, $\Delta n=3$ )	
18241.68	0.0793	H(n=111, $\Delta n=4$ )		19591.08	0.8888	H(n=69, $\Delta n=1$ )	
18249.78	0.0148	He(n=111, $\Delta n=4$ )		19599.08	0.0911	He(n=69, $\Delta n=1$ )	
18285.50	0.012	NH <sub>3</sub> (10,7)		19609.78	0.0177	U19610.0	NH <sub>2</sub> CHO?
18294.20	0.007	U18294.2		19621.56	0.0165	H(n=135, $\Delta n=8$ )	
18299.5	0.008	U18299.5		19682.50	0.012	U19682.5	
18306.3	0.005	U18306.3		19692.50	0.011	U19692.5	
18320.7	0.006	U18320.7		19746.98	0.0130	H(n=123, $\Delta n=6$ )	
18327.55	0.104	H(n=101, $\Delta n=3$ )		19757.50	0.007	NH <sub>3</sub> (6,3)	
18335.00	----	He(n=101, $\Delta n=3$ )		19771.50	0.015	U19771.5?	uncertain - near clean area of double line
18343.10	0.28	C <sub>2</sub> H <sub>2</sub> (1 <sub>10</sub> -1 <sub>01</sub> )	emission and absorption	19775.97	0.045	H(n=108, $\Delta n=4$ )	
18347.42	0.0279	H(n=119, $\Delta n=5$ )		19777.45	----	H(n=116, $\Delta n=5$ )	blended with $\Delta n=4$ line
18360.50	0.007	U18360.5		19838.35	0.005	NH <sub>3</sub> (5,1)	
18368.0	0.006	U18368.0		19967.53	0.0315	CH <sub>3</sub> OH (2 <sub>1</sub> -3 <sub>0</sub> )E1	
18371.0	0.004	T18371.0		19974.50	0.007	U19974.5	
18379.6	0.005	U18379.6		19978.18	0.2307	H(n=86, $\Delta n=2$ )	
18383.3	0.005	U18383.3		19986.41	0.0257	He(n=86, $\Delta n=2$ )	
18391.50	0.006	NH <sub>3</sub> (6,1)		20036.29	0.1015	H(n=98, $\Delta n=3$ )	
18400.36	0.0301	H(n=126, $\Delta n=6$ )	CH <sub>3</sub> CN?	20044.75	0.0099	He(n=98, $\Delta n=3$ )	
18402.80	0.005	H(n=138, $\Delta n=8$ )		20051.81	0.0143	H(n=134, $\Delta n=8$ )	blended with H(n=148, $\Delta n=11$ )
18413.78	0.0134	<sup>13</sup> C CCH <sub>3</sub> 1 <sub>10</sub> -1 <sub>01</sub>	off-axis Isotopomer	20064.21	0.0088	U20064.2	H(n=152, $\Delta n=12$ )?
18422.00	0.0120	U18422.0		20068.32	0.0097	H(n=139, $\Delta n=9$ )	
18477.82	0.0143	H(n=143, $\Delta n=9$ )		20124.3	0.006	T20124.3	
18485.07	0.0164	U18485.0		20127.78	0.009	T20128.0	
18494.24	0.0141	CH <sub>3</sub> SH (18 <sub>2</sub> -17 <sub>2</sub> )	may also be present in TMC-1	20168.48	0.0103	U20168.5	
18499.45	0.5243	NH <sub>3</sub> (9,6)		20171.03	0.0146	CH <sub>3</sub> OH (11 <sub>1</sub> -10 <sub>2</sub> )A+	
18504.07	0.044	T18504.0		20203.31	0.0067	U20203.3	
18528.00	0.023	H(n=132, $\Delta n=7$ )		20225.28	0.0397	H(n=122, $\Delta n=6$ )	
18586.06	0.0117	U18586.1		20272.30	0.014	H(n=128, $\Delta n=7$ )	
18626.0	0.007	T18626.0		20281.00	0.013	U20281.0	
18638.5	0.005	HC <sub>3</sub> N (J=7-6)		20287.20	0.025	H(n=115, $\Delta n=5$ )	
18645.30	0.0105	T18645.3		20292.0	0.006	T20292.0	
18661.12	0.2372	H(n=88, $\Delta n=2$ )		20325.50	0.047	H(n=107, $\Delta n=4$ )	
18668.76	0.0215	He(n=88, $\Delta n=2$ )		20331.5	0.011	T20331.5	
18698.16	0.0085	U18698.2		20371.13	0.0084	NH <sub>3</sub> (5,2)	
18729.12	0.0207	U18729.0		20455.50	0.010	T20455.5	
18734.93	0.062	H(n=110, $\Delta n=4$ )		20461.78	1.0533	H(n=68, $\Delta n=1$ )	
18746.0	0.005	T18746.0		20470.14	0.0905	He(n=68, $\Delta n=1$ )	
18758.0	0.015	T18758.0		20494.45	0.0176	H(n=133, $\Delta n=8$ )	blended with H(n=138, $\Delta n=9$ )
18769.15	1.0432	H(n=70, $\Delta n=1$ )		20501.5	0.008	U20501.5	
18776.76	0.0961	He(n=70, $\Delta n=1$ )		20652.94	0.0806	H(n=97, $\Delta n=3$ )	
18793.92	0.0209	U18794.0		20661.43	0.0183	He(n=97, $\Delta n=3$ )	
18796.86	0.0087	H(n=137, $\Delta n=8$ )		20683.32	0.1997	H(n=85, $\Delta n=2$ )	
18808.35	0.0424	H(n=118, $\Delta n=5$ )	confused with NH <sub>3</sub> (8,5)	20691.94	0.0181	He(n=85, $\Delta n=2$ )	
18817.66	0.0168	U18817.7	He(n=118, $\Delta n=5$ )? HCO (2,2)?	20707.80	0.011	U20707.8	
18835.12	0.0287	H(n=125, $\Delta n=6$ )		20718.87	0.0219	H(n=121, $\Delta n=6$ )	confused with NH <sub>3</sub> (8,6)
18858.79	0.0087	H(n=142, $\Delta n=9$ )		20723.5	0.017	U20723.5	
18864.65	0.0154	U18864.5	CH <sub>2</sub> <sup>13</sup> CHCN?	20728.67	0.0144	U20728.7	
				20735.4	0.0025	NH <sub>3</sub> (9,7)	

TABLE 1—Continued

Frequency (MHz)	$T_A$ (K)	Identification	Comments
20737.2	0.008	T20737.2	
20742.55	0.0165	H(n=127, $\Delta n=7$ )	
20746.5	0.010	T20746.5	
20751.05	0.0132	H(n=142, $\Delta n=10$ )	
20765.80	0.014	U20765.8	
20769.5	0.006	T20769.5	
20790.00	0.007	U20790.0	
20792.66	0.0111	H <sub>2</sub> C <sub>3</sub> 1 <sub>01</sub> -0 <sub>00</sub>	
20793.6	0.003	C <sub>6</sub> H J=7.5-6.5	$\lambda$ -doublet in $\Pi_{3/2}$ ladder
20804.20	0.010	NH <sub>3</sub> (7,5)	
20814.25	0.0422	H(n=114, $\Delta n=5$ )	
20823.00	0.005	He(N=114, $\Delta n=5$ )	
20838.20	0.006	U20838.2	
20847.50	0.003	U20847.5	HNO <sub>3</sub> ?
20851.80	0.007	NH <sub>3</sub> (10,8)	
20858.02	0.0108	H(n=146, $\Delta n=11$ )	
20878.00	0.006	U20878.0	
20895.71	0.0577	H(n=106, $\Delta n=4$ )	
20909.00	0.007	CH <sub>3</sub> OH (16 <sub>4</sub> -15 <sub>3</sub> )E2	
20932.55	0.0102	H(n=137, $\Delta n=9$ )	
20941.9	0.003	C <sub>6</sub> H J=7.5-6.5	$\lambda$ -doublet in $\Pi_{1/2}$ ladder
20951.42	0.015?	H(n=132, $\Delta n=8$ )	
20951.5	0.015	T20951.5	
20999.79	0.0088	U20999.8	
21143.18	0.0168	U21143.2	
21228.60	0.0130	H(n=120, $\Delta n=6$ )	blended with H(n=126, $\Delta n=7$ )
21231.00	-0.013	U21231.0	questionable-difficult to clean
21285.20	0.0140	NH <sub>3</sub> (5,3)	
21295.19	0.082	H(n=96, $\Delta n=3$ )	
21304.10	0.007	He(n=96, $\Delta n=3$ )	
21322.50	-0.010	U21322.5	H <sup>15</sup> NCO (1 <sub>10</sub> -0 <sub>00</sub> )?
21359.91	0.0306	H(n=113, $\Delta n=5$ )	
21368.51	0.0079	He(n=113, $\Delta n=5$ )	
21384.79	0.6975	H(n=67, $\Delta n=1$ )	
21393.54	0.0747	He(n=67, $\Delta n=1$ )	
21422.12	0.1749	H(n=84, $\Delta n=2$ )	
21430.68	0.0188	He(n=84, $\Delta n=2$ )	
21440.779	0.008	T21440.8	HC <sub>3</sub> N 1V7?
21447.8	0.005	U21447.8	
21453.93	-0.0097	U21454.0	
21470.4	0.007	U21470.4	
21487.33	0.0496	H(n=105, $\Delta n=4$ )	
21494.92	0.0095	He(n=105, $\Delta n=4$ )	
21546.94	0.0059	U21547.0	
21559.6	0.003	T21559.8	
21569.5	0.0075	U21569.5	
21576.5	0.0045	U21576.5	
21582.6	0.003	U21582.6	
21587.14	-0.0646	C <sub>3</sub> H <sub>2</sub> (2 <sub>20</sub> -2 <sub>11</sub> )	
21592.1	0.004	U21592.1	
21595.8	0.005	U21595.8	(HDCO 28 <sub>3,23</sub> -28 <sub>5,24</sub> )?
21598.4	0.006	U21598.4	
21606.30	0.005	U21606.3	
21615.5	0.003	U21615.5	
21622.5	0.006	H(n=140, $\Delta n=10$ )	
21703.16	0.0208	NH <sub>3</sub> (4,2)	
21707.05	0.0086	H(n=144, $\Delta n=11$ )	
21715.8	0.008	U21715.8	
21727.19	0.0108	H(n=125, $\Delta n=7$ )	
21755.10	0.0144	H(n=119, $\Delta n=6$ )	
21846.89	0.0119	H(n=135, $\Delta n=9$ )	
21903.80	0.012	H(n=130, $\Delta n=8$ )	
21925.00	0.030	H(n=112, $\Delta n=5$ )	
21964.30	0.085	H(n=95, $\Delta n=3$ )	
22005.5	0.005	T22005.5	
22014.0	0.010	T22014.0	

NOTES.—For known lines the listed frequencies are rest frequencies. For unidentified lines the listed frequencies represent the centre of the line assuming an LSR velocity of 60 km s<sup>-1</sup>.

to allow frequency switching but wide enough to allow the use of relatively wide channel widths, the 18.343 GHz line of C<sub>3</sub>H<sub>2</sub> may be more easily detected in this source than in any other source in the sky. This is of some interest since strong C<sub>3</sub>H<sub>2</sub>, like HC<sub>3</sub>N (Cox, Walmsley, & Güsten 1989) is more usually found to be associated with cool sources. Here, the antenna temperature obtained for C<sub>3</sub>H<sub>2</sub> (1<sub>10</sub>-1<sub>01</sub>) is at least two orders of magnitude stronger than the antenna temperature measured for HC<sub>3</sub>N. A feature was also detected at the position of its off-axis <sup>13</sup>C isotopomer which gave an antenna temperature ratio  $T_A(\text{C}_3\text{H}_2)/T_A(\text{C}_2^{13}\text{CH}_2) \approx 38$ .

In W51 the carbon-chain molecules are relatively weak, with HC<sub>3</sub>N the only cyanopolyne detected conclusively. Although there is a feature at the expected position of HC<sub>3</sub>N ( $J = 7-6$ ), nothing is evident at the position of the  $J = 8-7$  line, although this may be due to a combination of increased atmospheric absorption and decreased receiver sensitivity. In any event, an upper limit on the HC<sub>3</sub>N/HC<sub>5</sub>N antenna temperature ratio is  $\sim 8$  which, as in Orion, is much higher than found in cooler sources.

Also curious is the possibility that C<sub>6</sub>H  $J = 7.5-6.5$  ( $\Pi_{3/2}$   $\lambda$ -doublet) may have been detected (Fig. 3) while C<sub>4</sub>H was not. Although C<sub>4</sub>H falls in an insensitive portion of the spectrum and the C<sub>6</sub>H doublet is in a long integration region, the C<sub>4</sub>H/C<sub>6</sub>H antenna temperature ratio would be close to unity if C<sub>6</sub>H has been detected. The fact that the C<sub>6</sub>H  $\Pi_{1/2}$  doublet is not seen is not surprising since C<sub>6</sub>H has an inverted <sup>2</sup> $\Pi$  ground state and the  $\Pi_{3/2}$  doublet is expected to be stronger.

A list of those molecules that have transitions that are coincident with survey features is given in Table 2. Because there was evidence after the initial integration period that some known molecules might be present, we carried out additional integration to improve the signal-to-noise ratio. Some examples are the off-axis isotopomer of cyclic C<sub>2</sub><sup>13</sup>CH<sub>2</sub> and its linear form H<sub>2</sub>CCC. However, in the long integration spectrum the (1<sub>0,1</sub>-0<sub>0,0</sub>) line of H<sub>2</sub>CCC (Vrtilek et al. 1990) is only one channel wide and must be considered tentative until further observations are obtained. Although weak features appear at the locations of both ortho lines of H<sub>2</sub>CCCC (Cernicharo et al. 1991), no attempt has yet been made to confirm them since their frequencies were not known when the observations were made. There is no evidence of a feature at the position of para H<sub>2</sub>CCCC.

The strength of the cyclic C<sub>3</sub>H<sub>2</sub>(1<sub>10</sub>-1<sub>01</sub>) transition, combined with its relatively broad Doppler width makes W51 a good source in which to search for propargylene, the nearly linear version of this molecule (see DeFrees & MacLean 1986) whose constants so far have not been measured in the laboratory. Although a group of lines near 20.12 GHz was tentatively assigned to this molecule by Thaddeus, Vrtilek, & Gottlieb (1985), they were later shown by Saito et al. (1988) to be due to the CH<sub>2</sub>CN radical.

Since three transitions of CH<sub>3</sub>OH have been detected, its presence in W51 is assumed to be confirmed. The existence of CH<sub>3</sub>SH is less certain, however, since there are no other transitions in the observed band. If this transition is detectable in W51 it would also be expected to be detectable in TMC-1 and attempts to confirm this line in TMC-1 show a weak feature at the correct position. Further integration will be required in W51, however, before a detection can be claimed.

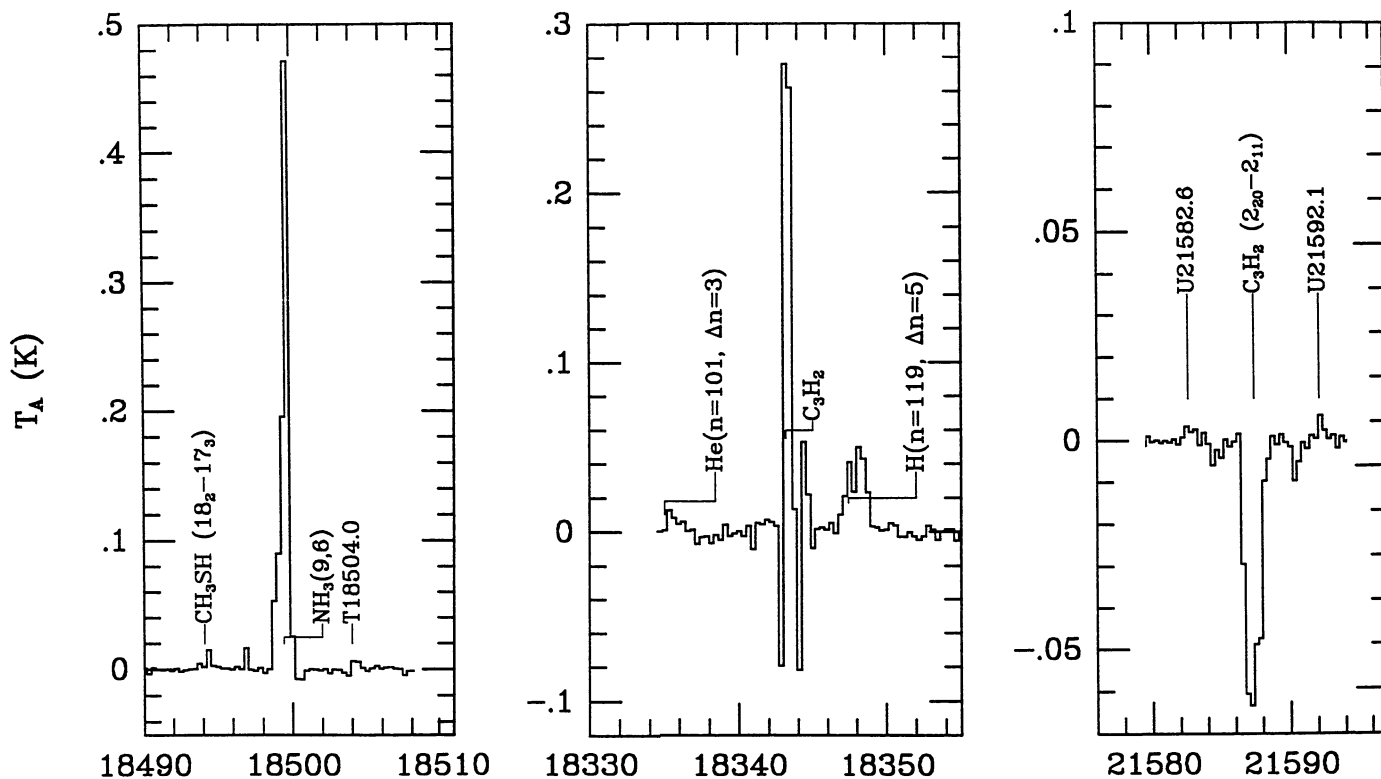


FIG. 2.—Molecular lines that are off-scale in Fig. 1 replotted so their full extent is visible. The strong masering line of  $\text{NH}_3(9,6)$  is shown in Fig. 2a and may show a slight extension to higher velocities in its wings. The absorption features on each side of the  $\text{C}_3\text{H}_2(1_{10}-1_{01})$  line in Fig. 2b have been reported previously (Madden et al. 1989). The horizontal scale gives the frequency in MHz.

### 3. AMMONIA IN W51

Many extensive observations of ammonia in W51 have been carried out in the past (see, e.g., Ho et al. 1983; Madden et al. 1986, 1989; Mauersberger et al. 1985, 1986, 1987; Brown & Cragg 1991; Pratap et al. 1991; Wilson, Johnson, & Henkel 1990), and it is of interest to compare our data with those of previous investigators. Although there are 25 ammonia transitions falling inside the survey range, several are confused with hydrogen recombination lines or occur at the intersection between two banks and cannot be “cleaned” properly. Also, some occur at frequencies that lie in areas of poor receiver response. As a result only 15 transitions fall in useable areas and, of those, 11 were detected as listed in Table 3. In Figure 4 we present these data in an excitation plot where  $\log [3kW/8\pi^3\nu\mu^2S]$  is plotted versus the excitation energy (where  $W = T_b\Delta V_{1/2}$  and  $S = K^2(2J+1)/[J(J+1)]$ ). The data have been corrected both for the change in telescope efficiency and atmospheric absorption with frequency. Although there appears at first glance to be a considerable amount of scatter in the data, when points of constant  $(J-K)$  are joined, it can be seen from the slopes of these lines, at any given excitation energy, that the excitation temperature for this molecule increases with  $J-K$ . There may also be some evidence that the curves of constant  $J-K$  depart from a straight line indicating that the excitation temperature for this molecule also increases with  $J$ . This implies that there is a range of gas temperatures in the line-of-sight (see, e.g., Evans, Lacy, & Carr 1991). The increase in excitation temperature with  $J-K$ , for  $J-K$  values between 2

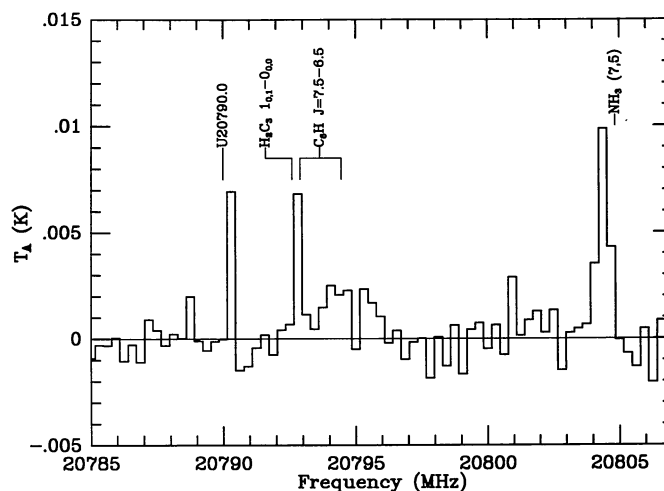


FIG. 3.—Spectral plot of the region near the  $\text{C}_6\text{H } J=7.5-6.5$   $\lambda$ -doublet in the  $\Pi_{3/2}$  ladder. The LSR velocity assumed was  $60 \text{ km s}^{-1}$ , and for most molecules it is known to be  $57 \text{ km s}^{-1}$ , except for  $\text{NH}_3$  where the mean velocity found was  $63 \pm 3 \text{ km s}^{-1}$ . There is no evidence of the  $\Pi_{1/2}$  doublet. It is expected to be weaker since the molecule has an inverted  ${}^2\Pi$  ground state, and also it is located in a region of the spectrum obtained with less than half the integration used in the above spectrum. The horizontal scale is in MHz.

TABLE 2  
LIST OF MOLECULES COINCIDENT WITH FEATURES OBSERVED IN W51

Molecule	Transition	Comments
H <sub>2</sub> C <sub>4</sub> .....	2 <sub>1,2</sub> -1 <sub>1,1</sub> ; 2 <sub>1,1</sub> -1 <sub>1,0</sub>	...
NH <sub>3</sub> .....	(7,3), (10,7), (9,6) (6,1), (6,2), (6,3), (5,2), (7,5), (10,8), (5,3), (4,2)	...
HC <sub>3</sub> N .....	<i>J</i> = 2-1	...
HC <sub>5</sub> N .....	<i>J</i> = 7-6	...
C <sub>3</sub> H <sub>2</sub> .....	(1 <sub>10</sub> -1 <sub>01</sub> ), (2 <sub>20</sub> -2 <sub>11</sub> )	...
CC <sup>13</sup> CH <sub>2</sub> .....	(1 <sub>10</sub> -1 <sub>01</sub> ) off-axis isotopomer	...
CH <sub>3</sub> SH .....	(18 <sub>2</sub> -17 <sub>3</sub> )	...
CH <sub>3</sub> OH .....	(2 <sub>1</sub> -3 <sub>0</sub> )E1, (11 <sub>1</sub> -10 <sub>2</sub> )A+, (16 <sub>-4</sub> -15 <sub>-5</sub> )E2	...
H <sub>2</sub> C <sub>3</sub> .....	1 <sub>0,1</sub> -0 <sub>0,0</sub>	Needs to be confirmed
C <sub>6</sub> H .....	<i>J</i> = 7.5-6.5	Needs to be confirmed
HNO <sub>3</sub> .....	55 <sub>43,12</sub> -55 <sub>43,13</sub> )	Unlikely
H <sup>15</sup> NCO .....	(1 <sub>10</sub> -0 <sub>00</sub> )	Unlikely
HDCO .....	(28 <sub>5,23</sub> -28 <sub>5,24</sub> )	Unlikely
HCO .....	(2,2)?	...

TABLE 3  
AMMONIA LINES IN W51

Frequency (MHz)	<i>J</i> , <i>K</i>	<i>E</i> <sub>upper</sub> / <i>k</i> (K)	<i>T</i> <sub>b</sub> (K)	$\Delta V$ (km s <sup>-1</sup> )	<i>W</i> = <i>T</i> <sub>b</sub> $\Delta V$	<i>S</i> <sup>a</sup>	<i>X</i> <sup>b</sup>
18017.6 .....	7,3	738.83	0.028	10	28378.4	2.41	11.703
18285.5 .....	10,7	1304.84	0.0328	6	19654.1	9.35	10.948
18313.6 .....	14,11	2340.35	<0.0079	10	7861.6	16.70	10.300
18391.5 .....	6,1	594.81	0.016	10	16378.4	0.31	12.347
18499.5 .....	9,6	1091.68	1.459	10	1458703.0	7.6	12.904
18884.7 .....	6,2	578.97	0.017	10	16702.7	1.24	11.742
19756.7 .....	6,3	553.04	0.026	10	26250.0	2.79	11.566
19838.4 .....	5,1	423.42	<0.021	10	20797.3	0.37	12.345
20371.5 .....	5,2	409.02	0.027	10	26810.8	1.47	11.841
20735.5 .....	9,7	1022.55	0.009	10	8986.5	10.3	10.510
20804.8 .....	7,5	666.82	0.037	10	37297.3	6.7	11.316
20852.5 .....	10,8	1227.07	0.030	10	30270.3	12.2	10.963
21070.7 .....	11,9	1448.86	<0.012	10	11675.7	14.1	10.482
21285.3 .....	5,3	381.66	0.061	10	60540.5	3.3	11.824
21703.4 .....	4,2	265.00	0.094	10	94216.2	1.8	12.270

$$^a S = K^2(2J + 1)/[J(J + 1)].$$

$$^b X = \log(3kW/8\pi^3\nu\mu^2S).$$

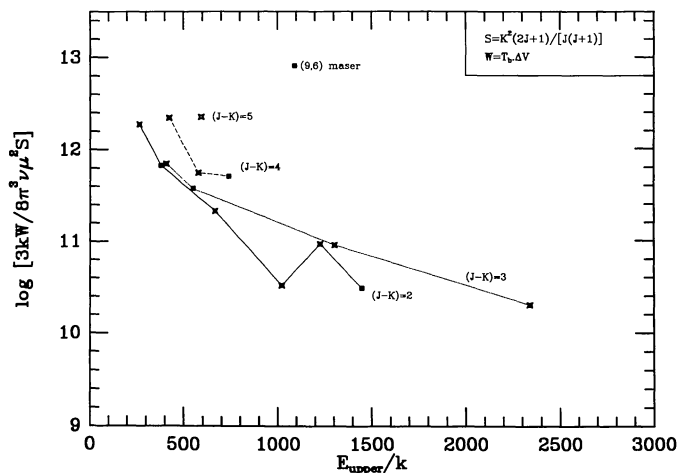


FIG. 4.—Excitation plot of ammonia lines in W51. Solid squares are ortho lines and stars represent para lines. Lines of constant *J* - *K* have been joined.

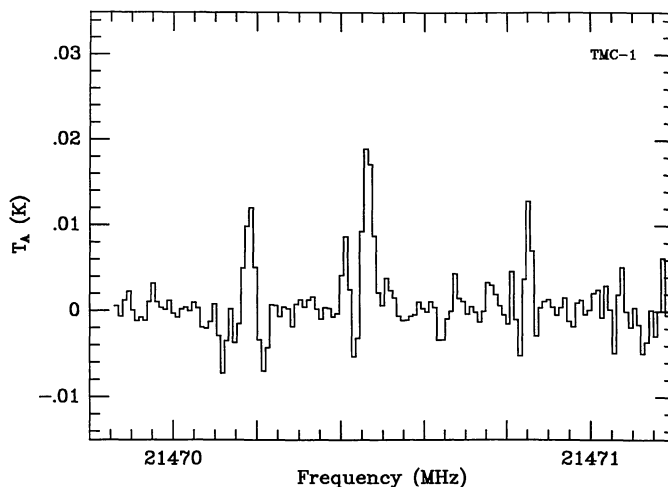


FIG. 5.—Spectrum of TMC-1 at 21470.4 MHz showing a feature that is assumed to be produced by the same carrier as that seen in Fig. 1.

and 5, is an extension of the results of Mauersberger et al. (1987), who found an increase in rotational temperature for  $J - K$  between 0 and 2, for W51 IRS 2. The (9,6) masering line has been excluded in this instance. Although other transitions have been found previously to have masering components, these are usually very narrow and would be severely channel diluted by our coarse frequency resolution. There is no indication that the ortho and para lines behave differently.

#### 4. U-LINES DETECTED IN W51

Since the survey covered 4500 MHz, linear molecules with  $B_0 < 2250$  MHz could have 2 or more lines present. We therefore carried out a search for harmonic coincidences in both  $\Sigma$  and  ${}^2\Pi$  ground states over a range of  $J$ -values between 5 and 23 and  $9/2$  and  $47/2$ , respectively. Of the 100 lines included in the harmonic search, there were several which were found to exhibit near-harmonic relationships; however, most required large values of the distortion constant  $D$  to fit. Further observations of different transitions, or searches in other sources are necessary before the reality of these harmonic relationships

can be determined and meaningful rotational constants calculated. In parallel with the W51 survey we have already begun a program to search for the stronger  $U$ -lines in the cold dust cloud TMC-1. A positive result in a narrow-line source can give important information on hyperfine structure. One feature that has already been confirmed in TMC-1 is the line at 21470.4 MHz. We plan to continue this search in the future. The detected line is shown in Figure 5. Its carrier is as yet unidentified but the spectrum may indicate the presence of associated hyperfine structure. Another possibility considered was that this line was due to the  $\text{SiC}_4$   $J = 7-6$  transition which is predicted to lie at 21472.77 MHz, but was not detected by us at that frequency in TMC-1. However, the large discrepancy between the predicted and observed frequency makes this an unlikely interpretation. Although the  $J = 6-5$  transition of  $\text{SiC}_4$  was also covered in W51, it was located at the intersection of two banks and would have been confused with a hydrogen  $\Delta n = 8$  line.

We wish to thank Kyle Hearfield for his help in preparing the spectra for publication.

#### REFERENCES

- Avery, L. W. et al. 1992, ApJ, 83, 363  
 Beckwith, S., & Zuckerman, B. 1982, ApJ, 255, 536  
 Bell, M. B., & Feldman, P. A. 1991, ApJ, 367, L33  
 Bell, M. B., Avery, L. W., MacLeod, J. M., & Matthews, H. E. 1992, ApJ, 400, 551  
 Bell, M. B., Avery, L. W., Watson, J. K. G., MacLeod, J. M., & Vallée, J. 1993, in preparation  
 Bogey, M., & Destombes, J. L. 1986, A & A, 159, L8  
 Brown, R. D., & Cragg, D. M. 1991, ApJ, 378, 445  
 Cernicharo, J., Gottlieb, C. A., Guélin, M., Killian, T. C., Thaddeus, P., & Vrtilék, J. M. 1991, ApJ, 368, L43  
 Cox, P., Walmsley, C. M., & Güsten, R. 1989, A & A, 209, 382  
 DeFrees, D. J., & MacLean, A. D. 1986, ApJ, 308, L31  
 Evans, N. J., Lacy, J. H., & Carr, J. S. 1991, ApJ, 383, 674  
 Fomalont, E. B., & Weliachew, L. 1973, ApJ, 181, 781  
 Genzel, R., Becklin, E. E., Wynn-Williams, C. G., Moran, J. M., Reid, M. J., Jaffe, D. T., & Downes, D. 1982, ApJ, 255, 527  
 Ho, P. T. P., Genzel, R., & Das, A. 1983, ApJ, 266, 596  
 Madden, S. C., Irvine, W. M., Matthews, H. E., Brown, R. D., & Godfrey, P. D. 1986, ApJ, 300, L79  
 Madden, S. C., Irvine, W. M., Matthews, H. E., Friberg, P., & Swade, D. A. 1989, AJ, 97, 1403  
 Martin, A. H. M. 1972, MNRAS, 157, 31  
 Mauersberger, R., Henkel, C., & Wilson, T. L. 1987, A & A, 173, 352  
 Mauersberger, R., Henkel, C., Wilson, T. L., & Walmsley, C. M. 1986, A&A, 162, 199  
 Mauersberger, R., Wilson, T. L., Batrla, W., Walmsley, C. M., & Henkel, C. 1985, A & A, 146, 168  
 Pratap, P., Menten, K. M., Reid, M. J., Moran, J. M., & Walmsley, C. M. 1991, ApJ, 373, L13  
 Saito, S., Yamamoto, S., Irvine, W. M., Ziurys, L. M., Suzuki, H., Ohishi, M., & Kaifu, N. 1988, ApJ, 334, L113  
 Thaddeus, P., Vrtilék, J. M., & Gottlieb, C. A. 1985, ApJ, 299, L63  
 Turner, B. E. 1989, ApJS, 70, 539  
 Wilson, T. L., Johnston, K. L., & Henkel, C. 1990, A & A, 229, L1  
 Vrtilék, J. M., Gottlieb, C. A., Gottlieb, E. W., Killian, T. C., & Thaddeus, P. 1990, ApJ, 364, L53